Electron spin diffusion in monolayer MoS$_2$

L. Wang and M. W. Wu[*]

Hefei National Laboratory for Physical Sciences at Microscale and Department of Physics,
University of Science and Technology of China, Hefei, Anhui 230026, China

Electron spin diffusion is investigated in monolayer MoS$_2$ in the absence of external electric and magnetic fields. The electron-impurity scattering, which is shown to play a negligible role in spin relaxation in time domain in this material, has a marked effect on the in-plane spin diffusion due to the anisotropic spin precession frequency in the spatial domain. With the electron-impurity and intervalley electron-phonon scatterings separately included in the scattering term, we study the intra- and intervalley diffusion processes of the in-plane spins by analytically solving the kinetic spin Bloch equations. The intravalley process is found to be dominant in the in-plane spin diffusion, in contrast to the case of spin relaxation in time domain, where the intervalley process can be comparable to or even more important than the intravalley one. For the intravalley process, we find that the in-plane spin diffusion is suppressed with the increase of impurity density but effectively enhanced by increasing electron density in both the degenerate and nondegenerate limits. We also take into account the electron-electron Coulomb scattering in the intravalley process. Interestingly, we find that in the nondegenerate limit, the intravalley spin-diffusion length presents an opposite trend in the electron-density dependence compared to the one with only electron-impurity scattering.

PACS number(s): 72.25.−b, 81.05.Hd, 71.10.−w, 71.70.Ej

I. INTRODUCTION

Monolayer MoS$_2$ has attracted much attention due to its promising applications in electronics [1–4], optoelectronics [3,5–14], valleytronics [9–17], and also spintronics [12,18–29]. For the application of spintronic devices, the suitable spin lifetime and spin-diffusion length are required [30–38]. This indicates the importance of the investigations on the spin relaxation and spin diffusion in this material.

Very recently, spin relaxation has been studied in monolayer MoS$_2$ [21,28,29]. Wang and Wu [29] calculated the in-plane spin-relaxation time of electrons due to the D'yakonov-Perel' [39] (DP) and Elliot-Yafet [40] (EY) mechanisms with the intra- and intervalley processes included. They pointed out that the DP mechanism, which results from the inhomogeneous broadening [41] together with any scattering process, dominates the spin relaxation. The inhomogeneous broadening is from the spin-orbit coupling (SOC) of the conduction band [29],

$$\boldsymbol{\Omega}^{\mu} = \left[2\lambda_c\mu + \mu A_1 k^2 + A_2\left(k_x^3 - 3k_x k_y^2\right)\right]\hat{\mathbf{z}}, \qquad (1)$$

where the z axis is perpendicular to the monolayer MoS$_2$ plane; λ_c, A_1, and A_2 are the strengths of the SOC; and $\mu = 1 (-1)$ represents the K (K′) valley. The first term of the SOC, which is momentum independent, only induces the intervalley DP spin relaxation, whereas the last two terms are momentum dependent, which lead to the intra- and intervalley spin-relaxation processes. In addition, as only the last term (i.e., negligible anisotropic cubic one) causes the DP spin relaxation with the electron-impurity scattering, the electron-impurity scattering is shown to play a marginal role in the spin relaxation [29].

In contrast to the spin relaxation in time domain, the inhomogeneous broadening in spin diffusion for in-plane spins is determined by the spin precession frequency [42,43],

$$\boldsymbol{\omega}^{\mu} = \frac{m^*\boldsymbol{\Omega}^{\mu}}{\hbar^2 k_x} = \frac{m^*}{\hbar^2}\left[\frac{2\lambda_c\mu}{k_x} + \frac{\mu A_1 k^2}{k_x} + A_2\left(k_x^2 - 3k_y^2\right)\right]\hat{\mathbf{z}}, \qquad (2)$$

when the spin diffusion is along the x axis. Here, m^* stands for the effective mass. Due to the existence of k_x^{-1}, all three terms become momentum dependent, which can induce the intra- and intervalley relaxations for in-plane spins along the diffusion. This is different from the case of the spin relaxation in time domain, as previously mentioned. In addition, k_x^{-1} also makes the first two terms (i.e., the leading ones) anisotropic. This suggests that the electron-impurity scattering may play an important role in the in-plane spin diffusion, which is greatly different from the case of the spin relaxation in time domain in monolayer MoS$_2$ [29], but similar to the case of the spin diffusion in semiconductors [42,43] and single-layer graphene [44].

As for the out-of-plane spins, the spin-diffusion length is infinite since the spin precession frequency $\boldsymbol{\omega}^{\mu}$ [see Eq. (2)] is along the out-of-plane direction. However, this is not the case in the presence of an out-of-plane electric field. Very recently, Bishnoi and Ghosh [45] investigated the out-of-plane spin diffusion with this electric field applied. They showed that the out-of-plane spins relax during the spin diffusion since the out-of-plane electric field induces a Rashba SOC, which provides an inhomogeneous broadening in the spatial domain for out-of-plane spins [42]. However, the Rashba SOC they used is incomplete according to the recent work by Kormányos *et al.* [46]. In addition, the electron-electron Coulomb and electron-impurity scatterings, which have been shown to play an important role in spin diffusion in semiconductors [42,43,47,48] and single-layer graphene [44], are absent in their work [45]. Moreover, they also overlooked the intervalley electron-phonon scattering, which is of crucial importance in

---

[*]Author to whom correspondence should be addressed: mwwu@ustc.edu.cn

spin relaxation in time domain [28,29]. It is noted that in addition to the out-of-plane electric field, an in-plane magnetic field can also lead to the out-of-plane spin relaxation along the spin diffusion [42,43,49]. This is because the in-plane magnetic field (**B**) gives rise to a spin precession frequency in the spatial domain as $m^* g \mu_B \mathbf{B}/(\hbar^2 k_x)$, which provides an inhomogeneous broadening for out-of-plane spins during the spin diffusion.

In this work, we investigate the electron spin diffusion in monolayer MoS$_2$ in the absence of the external electric and magnetic fields. As the contribution of the spin-flip scattering due to the EY mechanism is negligible [29,45], we only take into account the spin conserving scattering. With the electron-impurity (intervalley electron-phonon) scattering included, the intravalley (intervalley) diffusion process for in-plane spins is studied by analytically solving the kinetic spin Bloch equations (KSBEs) [50]. We find that the intravalley process dominates the in-plane spin diffusion, which is very different from the case of the spin relaxation in time domain in monolayer MoS$_2$ where the intervalley process can be comparable to or even more important than the intravalley one [29]. Moreover, it is shown that the in-plane spin-diffusion length decreases with the increase of the impurity density, but increases with increasing electron density in both the degenerate and nondegenerate limits. Very interestingly, with the electron-electron Coulomb scattering further taken into account, the in-plane spin-diffusion length shows an opposite electron-density dependence in the nondegenerate limit compared to the one with only the electron-impurity scattering.

This paper is organized as follows. In Sec. II, we introduce our model and the KSBEs. In Sec. III, we investigate the in-plane spin diffusion by analytically solving the KSBEs. We summarize in Sec. IV.

II. MODEL AND KSBEs

The effective Hamiltonian of the conduction band near the K (K′) point in monolayer MoS$_2$ reads

$$H_{\text{eff}}^{\mu} = \epsilon_{\mu \mathbf{k}} + \mathbf{\Omega}^{\mu} \cdot \boldsymbol{\sigma}/2, \tag{3}$$

according to the latest work by Wang and Wu [29]. Here, $\epsilon_{\mu \mathbf{k}} = \hbar^2 \mathbf{k}^2/(2m^*)$ with m^* representing the effective mass, $\mathbf{\Omega}^{\mu}$ is given in Eq. (1), and $\boldsymbol{\sigma}$ are the Pauli matrices.

We then construct the microscopic KSBEs [50] to investigate the electron spin diffusion in monolayer MoS$_2$. The KSBEs can be written as [50]

$$\partial_t \rho_{\mu \mathbf{k}}(x,t) = \partial_t \rho_{\mu \mathbf{k}}(x,t)|_{\text{coh}} + \partial_t \rho_{\mu \mathbf{k}}(x,t)|_{\text{scat}} + \partial_t \rho_{\mu \mathbf{k}}(x,t)|_{\text{dif}}, \tag{4}$$

with $\rho_{\mu \mathbf{k}}(x,t)$ being the density matrices of electrons at position x and time t. The diffusion terms are described as

$$\partial_t \rho_{\mu \mathbf{k}}(x,t)|_{\text{dif}} = -(\hbar k_x/m^*)\partial_x \rho_{\mu \mathbf{k}}(x,t) \tag{5}$$

by assuming that the spin diffusion is along the x axis [51]. The coherent terms $\partial_t \rho_{\mu \mathbf{k}}(x,t)|_{\text{coh}}$ can be found in Ref. [52]. As for the scattering terms $\partial_t \rho_{\mu \mathbf{k}}(x,t)|_{\text{scat}}$, we neglect the spin-flip ones due to the EY mechanism since the

contribution of the EY mechanism is negligible [29,45]. Here, we only include the spin conserving terms, i.e, the electron-electron Coulomb, electron-impurity, intravalley electron-acoustic phonon, electron-optical phonon, and also the intervalley electron-phonon [28,53] (electron-KTA, -KLA, -KTO, and -KLO) scatterings. Here, KTA, KLA, KTO and KLO correspond to the transverse acoustic, longitudinal acoustic, transverse optical, and longitudinal optical phonon modes at the K point, respectively. The detailed expressions of the above scattering terms are given in Ref. [52] and the scattering matrix elements are given in Ref. [28]. It is noted that the above scatterings, including the electron-impurity, electron-electron Coulomb, and intravalley electron-phonon ones, contribute to the intravalley spin-diffusion process, whereas the intervalley electron-phonon scattering induces the intervalley process.

III. SPIN DIFFUSION

A. Intravalley process

We first focus on the intravalley diffusion process for in-plane spins by simplifying the KSBEs with only the electron-impurity scattering included in the scattering term. By taking the steady-state condition, the Fourier components of the density matrix with respect to $\theta_{\mathbf{k}}$ are given by [54]

$$\frac{\hbar k}{2m^*} \partial_x \left[\rho_k^{l+1}(x) + \rho_k^{l-1}(x) \right]$$

$$= -\frac{i}{2\hbar} \left[(2\lambda_c + A_1 k^2)\sigma_z, \rho_k^l(x) \right] - \rho_k^l(x)/\tau_i^l, \tag{6}$$

where the valley index μ is neglected for the intravalley process. Here, $[A,B] \equiv AB - BA$ is the commutator, $\rho_k^l(x) = \int_0^{2\pi} d\theta_{\mathbf{k}} \rho_{\mathbf{k}}(x) e^{-il\theta_{\mathbf{k}}}/(2\pi)$, and $1/\tau_i^l = N_i m^* \int_0^{2\pi} d\theta_{\mathbf{k}} U_{\mathbf{q}}^2 (1 - \cos l\theta_{\mathbf{k}})/(2\pi \hbar^3)$ stands for the lth-order momentum scattering rate with $|\mathbf{q}| = \sqrt{2k^2(1 - \cos\theta_{\mathbf{k}})}$. N_i represents the impurity density and the electron-impurity scattering matrix element $U_{\mathbf{q}}^2 = [V_{\mathbf{q}}^{(0)}/\varepsilon(\mathbf{q})]^2$. $V_{\mathbf{q}}^{(0)} = 2\pi e^2/(\kappa q)$ denotes the two-dimensional bare Coulomb potential, with κ being the relative static dielectric constant [19]. The screening [55,56] $\varepsilon(\mathbf{q}) = 1 + 2m^* V_{\mathbf{q}}^{(0)}/(\pi \hbar^2)$ in the degenerate limit, whereas $\varepsilon(\mathbf{q}) = 1 + N_e V_{\mathbf{q}}^{(0)}/(k_B T)$ in the nondegenerate one, with N_e and k_B being the electron density and Boltzmann constant, respectively. It is noted that in recent experiments, the mobilities at room temperature are reported to be of the order of 0.1–10 cm^2 V^{-1} s^{-1} in monolayer MoS$_2$ on SiO$_2$ substrate [1,57,58]. By fitting to the mobilities in these experiments, one obtains the impurity densities (e.g., $N_i = 4.4 \times 10^{13}$ cm^{-2} corresponding to the mobility 10 cm^2 V^{-1} s^{-1}) [59]. With these impurity densities, the electron-impurity scattering is in the strong scattering limit (in time domain), i.e., $\langle |2\lambda_c + A_1 k^2| \rangle \tau_i^1/\hbar$ (e.g., $\sim 10^{-2}$ for $N_i = 4.4 \times 10^{13}$ cm^{-2}) $\ll 1$, with $\langle \cdot \rangle$ denoting the ensemble average. Then, one can only keep the lowest two orders of $|l|$ (i.e., 0, 1) and obtain [44,49,60]

$$\partial_x^2 \rho_k^0(x) = -[\sigma_z, [\sigma_z, \rho_k^0(x)]] c_1^2/2 + ic_2[\sigma_z, \rho_k^0(x)], \tag{7}$$

with $c_1 = (2\lambda_c + A_1 k^2)m^*/(\hbar^2 k)$ and $c_2 = (2\lambda_c + A_1 k^2)m^{*2}/(\hbar^3 k^2 \tau_i^1)$. By solving this equation under the boundary conditions, the steady-state spin vector $\mathbf{S}_k(x) = \text{Tr}[\rho_k^0(x)\boldsymbol{\sigma}]$ can be obtained.

Since the system is isotropic for in-plane spins, we choose the injected spin polarization along the x axis without losing generality. With the boundary condition $\mathbf{S}_k(0) = (S_k(0),0,0)$ and $\mathbf{S}_k(+\infty) = 0$, we have

$$S_k^x(x) = S_k(0) \cos\left(\omega_{\text{intra}}^{\text{in}} x\right) e^{-x/l_{\text{intra}}^{\text{in}}}, \qquad (8)$$

with

$$\omega_{\text{intra}}^{\text{in}} = \sqrt{\sqrt{c_1^4 + c_2^2} + c_1^2}, \qquad (9)$$

$$1/l_{\text{intra}}^{\text{in}} = \sqrt{\sqrt{c_1^4 + c_2^2} - c_1^2}. \qquad (10)$$

B. Intervalley process

We then turn to investigate the intervalley spin-diffusion process by analytically solving the KSBEs with the intervalley electron-phonon scattering included in the scattering term. Similar to the intravalley process, one obtains

$$\frac{\hbar k}{2m^*} \partial_x \left[\rho_{\mu k}^{l+1}(x) + \rho_{\mu k}^{l-1}(x) \right]$$
$$= -\frac{i(2\lambda_c + A_1 k^2)\mu}{2\hbar} \left[\sigma_z, \rho_{\mu k}^l(x) \right]$$
$$- \left[\rho_{\mu k}^l(x)/\tau_v^0 - \rho_{-\mu k}^l(x)/\tau_v^l \right], \qquad (11)$$

based on the elastic-scattering approximation [28,61,62]. Here, $1/\tau_v^l = (2N_{\text{ph}} + 1)m^* \int_0^{2\pi} d\theta_{\mathbf{k}} M_{\mathbf{q}}^2 \cos l\theta_{\mathbf{k}}/(2\pi\hbar^3)$ is the lth-order intervalley momentum scattering rate, with N_{ph} and $M_{\mathbf{q}}^2$ being the phonon number and the intervalley electron-phonon scattering matrix element, respectively. It is noted that differing from the electron-impurity scattering, the intervalley electron-phonon scattering is in the weak scattering limit (in time domain) according to the recent work by Wang and Wu [28], i.e., $\langle |2\lambda_c + A_1 k^2| \rangle |\tau_v^{0,1}|/\hbar \gg 1$. This indicates that high orders of $\rho_{\mu k}^l$ may be relevant in the intervalley process. For simplicity, we first retain the lowest two orders of $|l|$ (i.e., 0, 1) and obtain

$$\partial_x^2 \rho_{\mu k}^0(x) = -\left[\sigma_z, \left[\sigma_z, \rho_{\mu k}^0(x) \right] \right] c_1^2/2$$
$$+ i c_3 \mu \left[\sigma_z, 2\rho_{\mu k}^0(x) - \rho_{-\mu k}^0(x) c_4 \right], \qquad (12)$$

with $c_3 = (2\lambda_c + A_1 k^2)m^{*2}/(\hbar^3 k^2 \tau_v^0)$ and $c_4 = 1 - \tau_v^0/\tau_v^1$. From this equation together with certain boundary conditions, we can obtain the steady-state spin vector $\mathbf{S}_{\mu k}(x) = \text{Tr}[\rho_{\mu k}^0(x)\boldsymbol{\sigma}]$. Similar to the intravalley process, we also set the initial spin polarization along the x axis. Under the boundary condition that $\mathbf{S}_{\mu k}(0) = (S_k(0),0,0)$ and $\mathbf{S}_{\mu k}(+\infty) = 0$, we have

$$\sum_\mu S_{\mu k}^x(x) = 2S_k(0) \cos\left(\omega_{\text{inter}}^{\text{in}} x\right) e^{-x/l_{\text{inter}}^{\text{in}}}, \qquad (13)$$

where

$$\omega_{\text{inter}}^{\text{in}} = \sqrt{2}c_1, \qquad (14)$$

$$1/l_{\text{inter}}^{\text{in}} = c_3\sqrt{4 - c_4^2}/(\sqrt{2}c_1). \qquad (15)$$

With higher orders ($|l| > 1$) of $\rho_{\mu k}^l$ included, we find that the intervalley spin-diffusion length $l_{\text{inter}}^{\text{in}}$ varies slightly (not shown) [63].

C. Discussion and results

In the calculation, the effective mass $m^* = 0.38m_0$, with m_0 being the free electron mass [29]; the coefficients of the SOC are $\lambda_c = 1.5$ meV (Ref. [25]) and $A_1 = 417.94$ meV Å^2 [29]. The parameters related to the scattering matrix elements are given in Ref. [28]. With these parameters, we calculate the intra- and intervalley spin-diffusion lengths in both the degenerate and nondegenerate limits.

In the degenerate limit, the intra- and intervalley spin-diffusion lengths are given by $l_{\text{intra}}^{\text{in}}(k_F)$ and $l_{\text{inter}}^{\text{in}}(k_F)$ according to Eqs. (10) and (15), respectively. Here, k_F is the Fermi wave vector. To compare the relative importance between the intra- and intervalley processes in the spin diffusion, we calculate

$$\frac{l_{\text{intra}}^{\text{in}}(k_F)}{l_{\text{inter}}^{\text{in}}(k_F)} = \frac{c_3}{\sqrt{2}c_1}\sqrt{4 - c_4^2} \Big/ \sqrt{\sqrt{c_1^4 + c_2^2} - c_1^2}. \qquad (16)$$

As the electron-impurity scattering is in the strong scattering limit in time domain (i.e., $c_1^2 \ll c_2$) and the intervalley electron-phonon scattering is in the weak scattering limit in time domain (i.e., $c_1^2 \gg c_3$), we have $l_{\text{intra}}^{\text{in}}(k_F) \ll l_{\text{inter}}^{\text{in}}(k_F)$. This indicates that the intravalley process dominates the in-plane spin diffusion, which is very different from the case of the spin relaxation in time domain in monolayer MoS$_2$, where the intervalley process is shown to be comparable or even more important than the intravalley one [29]. In the following, we only investigate the spin diffusion due to the intravalley process according to Eqs. (8)–(10).

In the degenerate limit, the in-plane spin vector is given by $S_{k_F}^x(x)$ approximately according to Eq. (8). The steady-state spatial distribution of this spin signal $S_{k_F}^x(x)/S_{k_F}(0)$ with only the electron-impurity scattering included is plotted in Fig. 1. The impurity density is taken to be $N_i = 3 \times 10^{12}$ cm^{-2} so
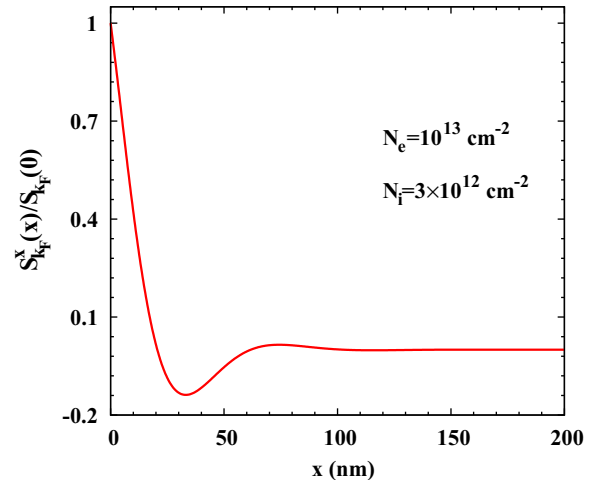

FIG. 1. (Color online) In-plane spin signal $S_{k_F}^x(x)/S_{k_F}(0)$ calculated from Eq. (8) with only the electron-impurity scattering included vs position x. The electron density $N_e = 10^{13}$ cm^{-2} and the impurity density $N_i = 3 \times 10^{12}$ cm^{-2}.

that the electron-impurity scattering is in the strong scattering limit in time domain. The corresponding mobility is of the order of 10^2 cm^2 V^{-1} s^{-1}, which is about one to two orders of magnitude larger than those reported in the experiments [1,57,58]. It is seen that the spin signal shows an obvious decay along the spin diffusion, which originates from the inhomogeneous broadening provided by the spin precession frequency in spatial domain [Eq. (2)]. In order to investigate the decay of the spin signal clearly, we focus on studying the spin-diffusion length $l_{\rm intra}^{\rm in}(k_F)$ according to Eq. (10) in the following.

In Fig. 2(a), we plot the electron-density dependence of the in-plane spin-diffusion length with the impurity density being $N_i = 3 \times 10^{12}$ cm^{-2}. We find that the spin-diffusion length due to the electron-impurity scattering (curve with $\times$) increases with the increase of the electron density. This can be understood as follows. The intravalley spin-diffusion length is approximately given by

$$l_{\rm intra}^{\rm in}(k_F) = 1/\sqrt{c_2} \qquad (17)$$

according to Eq. (10) under the condition that $c_1^2 \ll c_2$, as previously mentioned. When the electron density increases, the Fermi wave vector k_F increases, whereas the electron-impurity scattering rate $1/\tau_i^1$ decreases in the degenerate limit [52], leading to the decrease of c_2 and therefore the increase of the spin-diffusion length. In addition to the electron-impurity scattering, the electron-electron Coulomb scattering is also taken into account, whereas the intravalley electron-phonon scattering is neglected due to the negligible contribution [29]. As done in the spin relaxation in time domain [50,64], we calculate the in-plane spin-diffusion length according to Eq. (10) with the effective momentum scattering rate $1/\tau^* = 1/\tau_i^1 + 1/\tau_{\rm ee}$ replacing the one due to the electron-impurity scattering $1/\tau_i^1$. Here, $\tau_{\rm ee}^{-1} = (\pi/4)\ln(E_F/k_B T)k_B^2 T^2/(\hbar E_F)$ represents the momentum scattering rate due to the electron-electron Coulomb scattering, with E_F being the Fermi energy [64]. The results at $T = 50$, 75, and 100 K are shown in Fig. 2(a). By comparing these results with the one calculated with only the electron-impurity scattering (curve with $\times$), we find that the electron-impurity scattering plays a leading role in the in-plane spin diffusion. This is very different from the case of the spin relaxation in time domain in monolayer MoS$_2$, where the contribution of the electron-impurity scattering is marginal [29]. Moreover, we find that the intravalley spin-diffusion length decreases with the increase of the temperature when the electron density remains unchanged. This is because the electron-impurity scattering is insensitive to the temperature in the degenerate limit [52,62], whereas the electron-electron Coulomb scattering increases with increasing temperature in the degenerate limit [64], leading to the decrease of the spin-diffusion length as the temperature increases [see Eq. (17)].

In addition, we also investigate the impurity density dependence of the in-plane spin-diffusion length with the electron density $N_e = 10^{13}$ cm^{-2}, as shown in the inset of Fig. 2(a), with only the electron-impurity scattering included. It is seen that the spin-diffusion length decreases with the increase of the impurity density, which can be easily understood from Eq. (17).

Then we turn to the nondegenerate limit. The intra- and intervalley spin-diffusion lengths are calculated by $l_{\rm intra}^{\rm in}(k_T)$
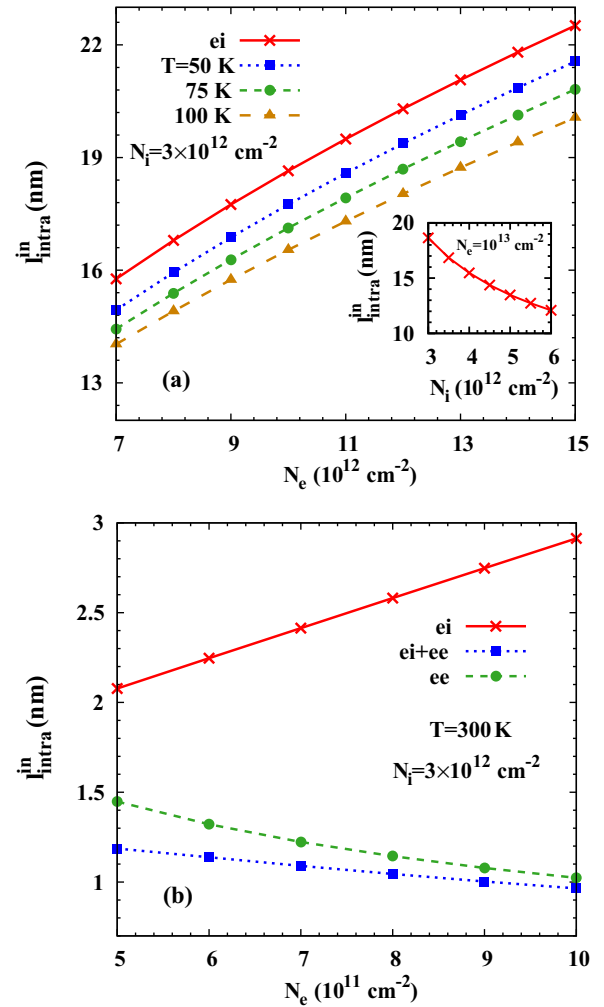

FIG. 2. (Color online) (a) Intravalley spin-diffusion length for in-plane spins $l_{\rm intra}^{\rm in}$ as a function of the electron density N_e in the degenerate limit. The curve with $\times$ stands for the calculation from Eq. (10) with only the electron-impurity scattering included, whereas the curves with ■, •, and ▲ represent the calculation based on Eq. (10) with the effective momentum scattering rate $1/\tau^*$ in place of $1/\tau_i^1$ at temperature $T = 50$, 75, and 100 K, respectively. The impurity density $N_i = 3 \times 10^{12}$ cm^{-2}. In addition, $l_{\rm intra}^{\rm in}$ due to the electron-impurity scattering as a function of the impurity density N_i with $N_e = 10^{13}$ cm^{-2} is shown in the inset. (b) $l_{\rm intra}^{\rm in}$ as a function of N_e in the nondegenerate limit. The curves with $\times$, •, and ■ stand for the calculation from Eq. (10) with the momentum scattering rate being $1/\tau_i^1$, $1/\tau_{\rm ee}$, and $1/\tau^*$, respectively. $N_i = 3 \times 10^{12}$ cm^{-2} and $T = 300$ K.

and $l_{\rm inter}^{\rm in}(k_T)$ according to Eqs. (10) and (15), respectively. Here, $k_T = \sqrt{2m^* k_B T}/\hbar$ stands for the "thermal" wave vector [64]. Similar to the degenerate-limit case, the in-plane spin diffusion in the nondegenerate limit is also dominated by the intravalley process. With the impurity density $N_i = 3 \times 10^{12}$ cm^{-2}, we calculate the electron-density dependence of $l_{\rm intra}^{\rm in}(k_T)$ due to the electron-impurity scattering and the result is shown in Fig. 2(b). We find that the intravalley spin-diffusion length increases with the increase of the electron density, which results from the decrease of $1/\tau_i^1$ due to the increase of the screening in the nondegenerate limit [28]. With

the effective momentum scattering rate $1/\tau^* = 1/\tau_i^1 + 1/\tau_{ee}$ instead of $1/\tau_i^1$, we also take into account the electron-electron Coulomb scattering. It is noted that differing from the case of the degenerate limit, $1/\tau_{ee} = 35.7 e^4 N_e /(\hbar \kappa^2 k_B T)$ in the nondegenerate limit [64]. It is seen that the spins relax faster along the spin diffusion with increasing electron density, which is opposite to the situation with only the electron-impurity scattering included. This can be understood as follows. As the electron density increases, the enhancement of $1/\tau_{ee}$ leads to the decrease of the intravalley spin-diffusion length due to the electron-electron Coulomb scattering (curve with ●), which suppresses the increase of $l_{\mathrm{intra}}^{\mathrm{in}}(k_T)$ contributed by the electron-impurity scattering.

It is noted that the feature of the spin diffusion is similar to the one of the spin relaxation in the weak scattering limit in time domain [50]. Specifically, the intravalley spin-diffusion length decreases with increasing the scattering. This is because the spin precession frequency in the spatial domain is proportional to k_x^{-1} [65], which gives strong inhomogeneous broadening along the spin diffusion. Similar behavior has also been shown in the case of spin diffusion in symmetric silicon quantum wells under an in-plane magnetic field [49] since the spin precession frequency in the spatial domain has similar momentum dependence [65].

IV. SUMMARY

In conclusion, we have investigated the electron spin diffusion in monolayer MoS$_2$ in the absence of the external electric and magnetic fields. The anisotropic spin precession frequency in the spatial domain leads to a marked contribution of the electron-impurity scattering in the in-plane spin diffusion. This is a great difference from the spin relaxation in time domain in monolayer MoS$_2$ where the contribution of the electron-impurity scattering is negligible. With the electron-impurity and intervalley electron-phonon scatterings separately included in the KSBEs, we analytically study the intra- and intervalley diffusions for in-plane spins. The intravalley process is shown to play a dominant role in the in-plane spin diffusion, which is different from the case of the spin relaxation in time domain in this material where the intervalley process can be comparable to or even more important than the intravalley one. In the dominant intravalley process, it is shown that the in-plane spin diffusion is suppressed by increasing impurity density, but enhanced with the increase of the electron density in both the degenerate and nondegenerate limits. Interestingly, with the electron-electron Coulomb scattering further included, a decrease of the spin-diffusion length is observed as the electron density increases in the nondegenerate limit.

[1] B. Radisavljevic, A. Radenovic, J. Brivio, V. Giacometti, and A. Kis, Nat. Nanotech. **6**, 147 (2011).

[2] Y. Zhang, J. Ye, Y. Matsuhashi, and Y. Iwasa, Nano Lett. **12**, 1136 (2012).

[3] Q. H. Wang, K. Kalantar-Zadeh, A. Kis, J. N. Coleman, and M. S. Strano, Nat. Nanotech. **7**, 699 (2012).

[4] A. Castellanos-Gomez, E. Cappelluti, R. Roldán, N. Agraït, F. Guinea, and G. Rubio-Bollinger, Adv. Mater. **25**, 899 (2013).

[5] A. Splendiani, L. Sun, Y. Zhang, T. Li, J. Kim, C.-Y. Chim, G. Galli, and F. Wang, Nano Lett. **10**, 1271 (2010).

[6] K. F. Mak, C. Lee, J. Hone, J. Shan, and T. F. Heinz, Phys. Rev. Lett. **105**, 136805 (2010).

[7] G. Eda, H. Yamaguchi, D. Voiry, T. Fujita, M. Chen, and M. Chhowalla, Nano Lett. **11**, 5111 (2011).

[8] T. Korn, S. Heydrich, M. Hirmer, J. Schmutzler, and C. Schüller, Appl. Phys. Lett. **99**, 102109 (2011).

[9] T. Cao, G. Wang, W. Han, H. Ye, C. Zhu, J. Shi, Q. Niu, P. Tan, E. Wang, B. Liu, and J. Feng, Nat. Commun. **3**, 887 (2012).

[10] H. Zeng, J. Dai, W. Yao, D. Xiao, and X. Cui, Nat. Nanotech. **7**, 490 (2012).

[11] K. F. Mak, K. He, J. Shan, and T. F. Heinz, Nat. Nanotech. **7**, 494 (2012).

[12] D. Xiao, G.-B. Liu, W. Feng, X. Xu, and W. Yao, Phys. Rev. Lett. **108**, 196802 (2012).

[13] G. Sallen, L. Bouet, X. Marie, G. Wang, C. R. Zhu, W. P. Han, Y. Lu, P. H. Tan, T. Amand, B. L. Liu, and B. Urbaszek, Phys. Rev. B **86**, 081301(R) (2012).

[14] D. Lagarde, L. Bouet, X. Marie, C. R. Zhu, B. L. Liu, T. Amand, P. H. Tan, and B. Urbaszek, Phys. Rev. Lett. **112**, 047401 (2014).

[15] T. Yu and M. W. Wu, arXiv:1401.0047.

[16] G. Wang, L. Bouet, D. Lagarde, M. Vidal, A. Balocchi, T. Amand, X. Marie, and B. Urbaszek, arXiv:1402.6009.

[17] M. M. Glazov, T. Amand, X. Marie, D. Lagarde, L. Bouet, and B. Urbaszek, arXiv:1403.0108.

[18] Z. Y. Zhu, Y. C. Cheng, and U. Schwingenschlögl, Phys. Rev. B **84**, 153402 (2011).

[19] T. Cheiwchanchamnangij and W. R. L. Lambrecht, Phys. Rev. B **85**, 205302 (2012).

[20] E. S. Kadantsev and P. Hawrylak, Solid State Commun. **152**, 909 (2012).

[21] H. Ochoa and R. Roldán, Phys. Rev. B **87**, 245421 (2013).

[22] H. Shi, H. Pan, Y.-W. Zhang, and B. I. Yakobson, Phys. Rev. B **87**, 155304 (2013).

[23] H. Rostami, A. G. Moghaddam, and R. Asgari, Phys. Rev. B **88**, 085440 (2013).

[24] F. Zahid, L. Liu, Y. Zhu, J. Wang, and H. Guo, AIP Adv. **3**, 052111 (2013).

[25] A. Kormányos, V. Zólyomi, N. D. Drummond, P. Rakyta, G. Burkard, and V. I. Fal'ko, Phys. Rev. B **88**, 045416 (2013).

[26] E. Cappelluti, R. Roldán, J. A. Silva-Guillén, P. Ordejón, and F. Guinea, Phys. Rev. B **88**, 075409 (2013).

[27] K. Kośmider and J. Fernández-Rossier, Phys. Rev. B **87**, 075451 (2013).

[28] L. Wang and M. W. Wu, Phys. Lett. A **378**, 1336 (2014).

[29] L. Wang and M. W. Wu, Phys. Rev. B **89**, 115302 (2014).

[30] Y. Nishikawa, A. Takeuchi, M. Yamaguchi, S. Muto, and O. Wada, IEEE J. Quantum Electron. **2**, 661 (1996).

[31] J. M. Kikkawa, I. P. Smorchkova, N. Samarth, and D. D. Awschalom, Science **277**, 1284 (1997).

[32] J. M. Kikkawa and D. D. Awschalom, Nature (London) **397**, 139 (1999).

[33] I. Martin, Phys. Rev. B **67**, 014421 (2003).

[34] Z. Vörös, R. Balili, D. W. Snoke, L. Pfeiffer, and K. West, Phys. Rev. Lett. **94**, 226401 (2005).

[35] N. Tombros, C. Jozsa, M. Popinciuc, H. T. Jonkman, and B. J. van Wees, Nature (London) **448**, 571 (2007).

[36] S. Datta and B. Das, Appl. Phys. Lett. **56**, 665 (1990).

[37] J. Wunderlich, B. G. Park, A. C. Irvine, L. P. Zârbo, E. Rozkotová, P. Nemec, V. Novák, J. Sinova, and T. Jungwirth, Science **330**, 1801 (2010).

[38] H. C. Koo, J. H. Kwon, J. Eom, J. Chang, S. H. Han, and M. Johnson, Science **325**, 1515 (2009).

[39] M. I. D'yakonov and V. I. Perel', Zh. Eksp. Teor. Fiz. **60**, 1954 (1971) [Sov. Phys. JETP **33**, 1053 (1971)]; Fiz. Tverd. Tela (Leningrad) **13**, 3581 (1971) [Sov. Phys. Solid State **13**, 3023 (1972)].

[40] Y. Yafet, Phys. Rev. **85**, 478 (1952); R. J. Elliot, *ibid.* **96**, 266 (1954).

[41] M. W. Wu and C. Z. Ning, Eur. Phys. J. B **18**, 373 (2000); M. W. Wu, J. Phys. Soc. Jpn. **70**, 2195 (2001).

[42] J. L. Cheng and M. W. Wu, J. Appl. Phys. **101**, 073702 (2007).

[43] M. Q. Weng and M. W. Wu, Phys. Rev. B **66**, 235109 (2002); J. Appl. Phys. **93**, 410 (2003).

[44] P. Zhang and M. W. Wu, Phys. Rev. B **84**, 045304 (2011).

[45] B. Bishnoi and B. Ghosh, J. Comput. Electron. (2013), doi:10.1007/s10825-013-0547-7.

[46] A. Kormányos, V. Zólyomi, N. D. Drummond, and G. Burkard, Phys. Rev. X **4**, 011034 (2014).

[47] J. L. Cheng, M. W. Wu, and I. C. da Cunha Lima, Phys. Rev. B **75**, 205328 (2007).

[48] P. Zhang and M. W. Wu, Phys. Rev. B **84**, 014433 (2011).

[49] P. Zhang and M. W. Wu, Phys. Rev. B **79**, 075303 (2009).

[50] M. W. Wu, J. H. Jiang, and M. Q. Weng, Phys. Rep. **493**, 61 (2010).

[51] In the calculation, we neglect the marginal cubic term in Eq. (1). Therefore, the diffusion direction is chosen along the x axis without losing generality since the in-plane ones are identical.

[52] Y. Zhou and M. W. Wu, Phys. Rev. B **82**, 085304 (2010).

[53] K. Kaasbjerg, K. S. Thygesen, and K. W. Jacobsen, Phys. Rev. B **85**, 115317 (2012).

[54] It is noted that the cubic term in Eq. (1) is neglected here due to its marginal contribution to the spin diffusion contributed by the electron-impurity scattering, as previously mentioned. This is very different from the case of the spin relaxation in the time domain in monolayer MoS_2.

[55] G. D. Mahan, *Many-Particle Physics* (Plenum, New York, 1990).

[56] H. Haug and S. W. Koch, *Quantum Theory of the Optical and Electronic Properties of Semiconductors*, 4th ed. (World Scientific, Singapore, 2004).

[57] K. S. Novoselov, D. Jiang, F. Schedin, T. J. Booth, V. V. Khotkevich, S. V. Morozov, and A. K. Geim, Proc. Natl. Acad. Sci. USA **102**, 10451 (2005).

[58] A. Ayari, E. Cobas, O. Ogundadegbe, and M. S. Fuhrer, J. Appl. Phys. **101**, 014507 (2007).

[59] With a typical electron density $N_e = 10^{13}$ cm^{-2} [1,57], the impurity density $N_i = 4.4 \times 10^{13}$ cm^{-2} is obtained by fitting to the mobility 10 cm^2 V^{-1} s^{-1} at room temperature.

[60] B. Y. Sun and K. Shen, Solid State Commun. **151**, 1322 (2011).

[61] P. Zhang, Y. Zhou, and M. W. Wu, J. Appl. Phys. **112**, 073709 (2012).

[62] L. Wang and M. W. Wu, Phys. Rev. B **87**, 205416 (2013).

[63] The relative error between the intervalley spin-diffusion length with the orders $|l| \leqslant 1$ and $|l| \leqslant 2$ is about 18 % and the one between the intervalley spin-diffusion length with the orders $|l| \leqslant 2$ and $|l| \leqslant 3$ is about 6 %.

[64] M. M. Glazov and E. L. Ivchenko, Zh. Eksp. Teor. Fiz. **126**, 1465 (2004) [JETP **99**, 1279 (2004)].

[65] With the last term (i.e., the negligible one) in $\boldsymbol{\omega}^\mu$ [see Eq. (2)] neglected, the spin precession frequency in the spatial domain in monolayer MoS_2 is given by $(2\lambda_c + A_1 k^2)m^* \mu \hat{\mathbf{z}}/(\hbar^2 k_x)$, which is similar to the one provided by the external magnetic field [49] [i.e., $m^* g \mu_B \mathbf{B}/(\hbar^2 k_x)$].